processes

Article

Influence of Partition Wall Length on Inlet Flow Regime of a Pumping Station Arranged in Parallel with a Sluice Gate

Wei Shi [1,2], Fusheng Lv [2], Xianlei Yu [1], Xichen Wang [1], Chun Ni [1], Weigang Lu [2] and Lei Xu [2,*]

[1] Jiangsu Water Supply Co., Ltd., Eastern Route of S-to-N Water Diversion Project, Nanjing 210029, China; nsbdsw@126.com (W.S.); 19952183816@163.com (X.Y.); wangxichenhhu@163.com (X.W.); 17351932727@163.com (C.N.)

[2] College of Hydraulic Science and Engineering, Yangzhou University, Yangzhou 225009, China; mx120210616@stu.yzu.edu.cn (F.L.); wglu@yzu.edu.cn (W.L.)

* Correspondence: leixu@yzu.edu.cn

Abstract: When a sluice gate is arranged in parallel with pumping station units, biased flow occurs in the forebay when the units are operating. The transverse flow velocity in front of the channel inlet is relatively high, and, in severe cases, it may lead to the formation of suction vortices, impacting the stable operation of pump units. Taking the Liushan Pumping Station project of the Eastern Route of the South-to-North Water Diversion Project as a case study, this paper investigates the effect of the partition wall length on the inlet flow regime of pumping station units arranged in parallel with the sluice gate to reduce the transverse flow velocity in front of the channel inlet. Using numerical simulations, the inlet flow regimes for different partition wall lengths were compared. Moreover, the flow field distributions in the forebay under different operating conditions were analyzed alongside the transverse flow velocity in front of the channel inlet and the uniformity of flow velocity distribution in the section behind the channel inlet. Hydraulic model tests were then conducted to validate the simulation results. The results indicate that in the original design, there existed a vortex zone in the forebay in front of the inlet of the channel where the transverse flow was relatively high. However, the introduction of partition walls significantly reduced the transverse flow velocity in front of the inlet of the channel in the forebay. The optimal effect was achieved when the length of the partition wall was twice the width of the inlet channel. Furthermore, the uniformity of velocity distribution at the inlet of the channel increased by an average of 7.4%, leading to a substantial improvement in the inlet flow regime of the pumping station. The addition of partition walls in the forebay effectively resolved the issues related to the flow regime in the forebay, providing valuable references for similar engineering studies in the future.

Keywords: pumping station forebay; partition wall; inlet flow regime; numerical simulations; model tests

check for updates

Citation: Shi, W.; Lv, F.; Yu, X.; Wang, X.; Ni, C.; Lu, W.; Xu, L. Influence of Partition Wall Length on Inlet Flow Regime of a Pumping Station Arranged in Parallel with a Sluice Gate. *Processes* **2024**, *12*, 699. https://doi.org/10.3390/pr12040699

Academic Editor: Ireneusz Zbicinski

Received: 5 March 2024
Revised: 28 March 2024
Accepted: 28 March 2024
Published: 29 March 2024

1. Introduction

The pump station hydraulic system is shown in Figure 1. When the flow regime in the forebay of the pumping station is not uniform, it can affect the water inlet conditions of the pump. In severe cases, an air-entrained vortex may even be generated in front of the inlet channel, as shown in Figure 1a. Due to the influence of significant bias, a large area of reflux and vortex zones is generated in the forebay, as shown in Figure 1b. This is especially true for the pump station arranged in parallel with the sluice gate.

The combined arrangement of a sluice gate and a pumping station, known for its compact layout and minimal land occupancy, has been widely applied in water diversion and drainage projects, such as the Eastern Route of the South-to-North Water Diversion. However, it tends to produce complicated upstream and downstream water flow regimes during the operation of the hub. When the sluice gate and pumping station operate separately, the inflow tends to be biased towards one side. The flow direction of water entering the forebay of the pumping station forms an angle with the axis of the forebay, producing this biased flow within the forebay and a large backflow zone. This phenomenon further triggers adverse flow regimes, generating a surface vortex at the inlet of the pumping station. When the surface vortex is strong enough, it can carry gas into the pump, forming a surface suction cortex, which adversely affects the safe and stable operation of pumping units. Therefore, it is necessary to study the flow regimes in pumping stations combined with a sluice gate [1–3].

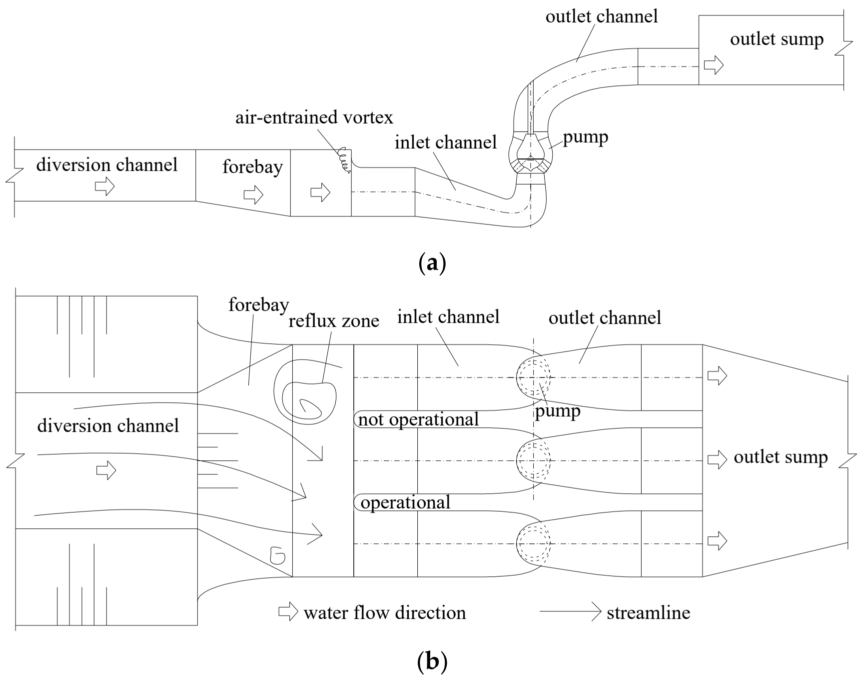

Figure 1. Hydraulic system of pumping station. (**a**) Elevation. (**b**) Layout plan.

The existing studies of the forebays of pumping stations mainly employed two methods, i.e., hydraulic model tests and numerical simulations [4–7]. For the pumping stations arranged in combination with a sluice gate, a diversion wall placed at the junction with the sluice gate significantly complicates the flow regime within the forebay. To improve the water flow conditions, various singular or combined rectification measures have been proposed [8–11]. Luo et al. [12] predicted the flow within the forebay during the operation of pumping units arranged in combination with a sluice gate and demonstrated that diversion piers can noticeably reduce the extent of the backflow zone. Wang et al. [13] used a combination of numerical simulation and engineering experiments to obtain the optimal inlet velocity in a circular forebay of a sandy river flow and improved the sustainability of engineering use. Song et al. [14] combined numerical simulations and model tests for laterally inflowing pumping stations and investigated five bias flow rectification measures, including Y-shaped diversion piers, T-shaped diversion piers, narrow-bottom hollow, wide-bottom and continuous diversion walls.

Xia et al. [15] conducted numerical simulations on an inverted T-shaped bottom sill placed within the forebay and analyzed how its geometry impacted the flow regime within the forebay and lateral flow velocities. Zhou et al. [16] studied the flow rectification within the forebay of laterally inflowing pumping stations using a single row of cylindrical pillars and demonstrated a reduction in the range of slope backflow zones and a more uniform approach to velocity at the inlet section. Yu et al. [17] optimized the structural design parameters of the bottom sill in the forebay of the pumping station based on computational fluid dynamics and the BPNN-GA algorithm. Luo et al. [18] performed numerical simulations emulating the flow field in the forebays of forward-flow and asymmetric pumping stations arranged in combination with a sluice gate and adjusted the flow regime within the forebay using rectification bottom sills and diversion piers. Xu et al. [19]. pointed out that attention should be paid to the safety and stability of the operation of the pumping station on both sides during actual operation.

Han et al. [20] demonstrated that placing rectification grid plates and bottom sills at bends and multiple diversion piers at the inlet of an inlet pool could significantly restrict the backflow zone within the forebay. Ying et al. [21] effectively improved the uniformity of the flow velocity distribution through a combined rectification method using pillars and bottom sills. Nasr Ahmed et al. [22] found that parabolic walls and partial diversion piers effectively improved the flow regime within the forebay of laterally inflowing pumping stations and the flow regime within the inlet pool. Zheng et al. [23] developed a combined rectification approach comprising bottom sills and diversion piers and revealed that the addition of bottom sills and the installation of diversion piers in the forebay allowed for secondary rectification, dispersing the inflow and producing more evenly distributed flow velocities among various units.

The flow regime within the forebay of a large-scale pumping station facility is influenced by various factors, such as the water level, flow velocity, operating combinations, bottom slope and divergence angle. The designs of different pumping station projects vary. As a result, the optimal measures required to improve the flow regime within the forebay may also differ. This study combines numerical simulations and model tests to investigate the flow regime within the forebay of the Liushan Pumping Station, which is arranged in parallel with a sluice gate and is part of Phase I of the Eastern Route of the South-to-North Water Diversion Project. The effect of the partition wall length on the inlet flow regime of pumping station units arranged in parallel with the sluice gate to reduce the transverse flow velocity in front of the channel inlet is studied.

2. Numerical Simulations and Model Tests

2.1. Numerical Simulations

2.1.1. Forebay Desing

The Liushan Pumping Station, Stage 7 hub of Phase I of the Eastern Route of the South-to-North Water Diversion, is located in the Bulao River section of the Beijng–Hangzhou Grand Canal. Its main purposes are transporting water from south to north and providing a navigation channel. In this engineering project, the pumping station is arranged in parallel with a sluice gate, as depicted in Figure 2. The station is equipped with five pump units. The design of the pumping flow is 125 m^3/s (including one spare pump), with the individual pumps designed for 31.25 m^3/s each. The streamwise length of the pumping station is 32.3 m, and the spanwise width is 43.32 m. The divergence angle of the diversion channel is 10°, while the bottom elevation of the station inlet is 13.5 m. The Liushan Regulating Sluice has five openings, each with a net width of 10 m, a weir crest elevation of 20.5 m, a streamwise length of 24.5 m and a spanwise width of 57.82 m. At the upstream and downstream of the piers of the regulating sluice, two diversion walls separate the sluice gate from the pumping station. The length of the upstream diversion wall is 40 m, while the downstream diversion wall is combined with the trash rack bridge, extending for 48 m. The distance between the trash rack bridge and the pumping station is 38 m, and the longitudinal axis of the downstream road bridge is 70.35 m away from the pumping station. The layout of the pumping station is illustrated in Figure 1.

The Liushan Pumping Station is arranged in parallel with its sluice gate, housing a total of five sets of pump units. There are various combinations of operating conditions, totaling 31, in which individual units are either switched on or off. To ensure the optimal flow regime in the forebay under different operational conditions, this study focuses on numerically simulating the flow field in the forebay for each operational condition at the minimum operational water level. Five representative operational combinations were selected for analysis, as listed in Table 1. For ease of the flow field description, the five pump units were sequentially labeled in the streamwise direction as #1–5 (Figure 1).

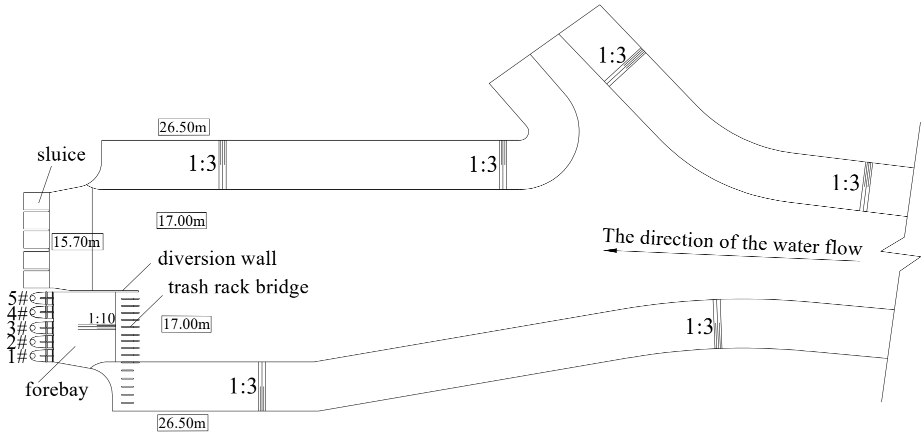

Figure 2. Combined arrangement of sluice gate and pumping station in the Liushan Pumping Station.

Table 1. Operating conditions selected for flow field simulations in pumping station forebay.

	Unit 1	Unit 2	Unit 3	Unit 4	Unit 5
Operating condition 1	On	Off	Off	Off	Off
Operating condition 2	On	On	Off	Off	Off
Operating condition 3	On	On	On	Off	Off
Operating condition 4	On	On	On	On	Off
Operating condition 5	On	On	On	On	On

The poor inlet flow regime in the forebay has an adverse impact on the safe and stable operation of the pump unit. Therefore, optimizing the flow state in the forebay is very important and necessary. The numerical simulation of the pumping station arranged in parallel with a sluice gate was carried out by the software Fluent. Measures were proactively taken to improve the inlet flow regime by introducing partition walls in the forebay. The width of each partition wall corresponds to the width of the separating pier between channels, while the length of each wall is a multiple of the width of the channel inlet, which is 7.1 m. Inlet widths of 0 times, 1 time, 2 times, 3 times and 4 times are used as partition wall length schemes. The adopted partition wall arrangements used walls of length 0.0 m, 7.1 m, 14.2 m, 21.3 m and 28.4 m, respectively. The wall end aligns with the abutment head of the trash rack bridge with a wall length of 48.3 m. The different arrangements of partition walls in the forebay are outlined in Table 2.

Table 2. Partition wall arrangements.

Arrangement	Partition Wall Length (m)	Planar View of Forebay	3D Drawing
1	0.0	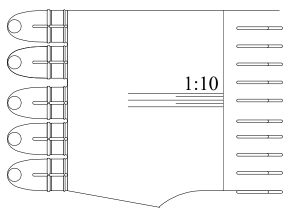	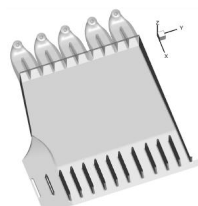
2	7.1	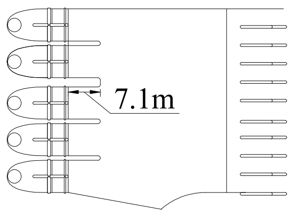	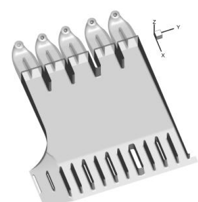

Table 2. *Cont.*

Arrangement	Partition Wall Length (m)	Planar View of Forebay	3D Drawing
3	14.2	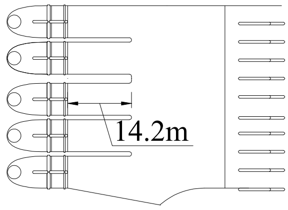	
4	21.3	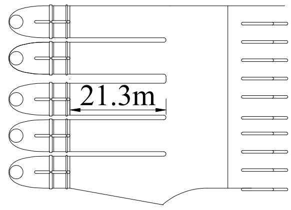	
5	28.4	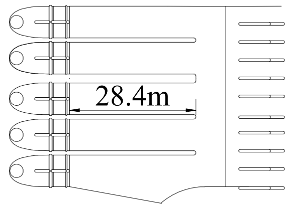	
6	48.3	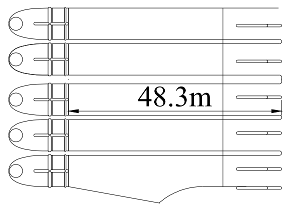	

2.1.2. Flow Governing Equations

The water in the forebay of the pumping station is considered a homogeneous and incompressible fluid with a constant viscosity. Its three-dimensional turbulent flow can be described using continuity and Navier–Stokes equations. In addition, two equations, namely for the turbulent kinetic energy k and its dissipation rate ε, need to be introduced to complete the problem description. The Reynolds averaged method is widely applied in numerical simulations of flow fields in the forebays of low-head pumping stations. The continuity and Navier–Stokes equations are as follows:

$$\frac{\partial \rho}{\partial t} + \rho \frac{\partial \overline{u_i}}{\partial x_i} = 0 \tag{1}$$

$$\rho \frac{\partial \overline{u_i}}{\partial t} + \rho \frac{\partial \overline{u_i u_j}}{\partial x_j} = -\frac{\partial \overline{p}}{\partial x_i} + \frac{\partial}{\partial x_j}\left[\mu\left(\frac{\partial \overline{u_i}}{\partial x_j} + \frac{\partial \overline{u_j}}{\partial x_i}\right) - \rho \overline{u_i' u_j'}\right] + F_i \tag{2}$$

where ρ is the density, kg/m^3; t is the time, s; $\overline{u_i}$ and $\overline{u_j}$ are the components of average velocity, m/s; x_i and x_j are the coordinates; $\overline{p}$ is the average pressure, Pa; μ is the dynamic viscosity coefficient, N·s/m^2; F_i is the component of volumetric force in x_i-direction; and $-\rho\overline{u_i' u_j'}$ is the Reynolds stress.

To complement the governing equations, the Boussinesq assumption is introduced, expressing Reynolds stress as a function of turbulent viscosity μ_t:

$$-\rho\overline{u_i' u_j'} = \mu_t\left(\frac{\partial \overline{u_i}}{\partial x_j} + \frac{\partial u_j}{\partial x_i}\right) - \frac{2}{3}\left(\rho k + \mu_t \frac{\partial \overline{u_i}}{\partial x_i}\right)\delta_{ij} \tag{3}$$

where k is the turbulent kinetic energy, δ_{ij} is the Kronecker delta, and ε is the turbulent kinetic energy dissipation rate.

Numerous numerical simulation results indicate that the RNG $k-\varepsilon$ turbulence model can accurately describe the three-dimensional flow field in the forebay [5,6,12,13]. The equations for k and ε adopted in this model are as follows:

$$\rho\frac{\partial k}{\partial t} + \rho\frac{\partial k\overline{u_i}}{\partial x_i} = \frac{\partial}{\partial x_j}\left[\left(\mu + \frac{\mu_t}{\sigma_k}\right)\frac{\partial k}{\partial x_j}\right] + G_k - \rho\varepsilon \tag{4}$$

$$\rho\frac{\partial \varepsilon}{\partial t} + \rho\frac{\partial \varepsilon\overline{u_i}}{\partial x_i} = \frac{\partial}{\partial x_j}\left[\left(\mu + \frac{\mu_t}{\sigma_\varepsilon}\right)\frac{\partial \varepsilon}{\partial x_j}\right] + \frac{C_{1\varepsilon}\varepsilon}{k}G_k - C_{2\varepsilon}\rho\frac{\varepsilon^2}{k} \tag{5}$$

where $G_k = \mu_t\left(\frac{\partial \overline{u_i}}{\partial x_j} + \frac{\partial \overline{u_j}}{\partial x_i}\right)\frac{\partial \overline{u_i}}{\partial x_j}$ is the generation term of turbulent kinetic energy, $C_{1\varepsilon} = 1.42 - \frac{\eta(1-\eta/\eta_0)}{1+\beta\eta^3}$, $C_{2\varepsilon} = 1.68$, $\sigma_k = 0.7179$ and $\sigma_\varepsilon = 0.7179$ are empirical constants, with $\eta = (2E_{ij}\cdot E_{ij})^{1/2}\frac{k}{\varepsilon}$, $E_{ij} = \frac{1}{2}\left(\frac{\partial \overline{u_i}}{\partial x_j} + \frac{\partial \overline{u_j}}{\partial x_i}\right)$, $\eta_0 = 4.377$ and $\beta = 0.012$.

2.1.3. Boundary Conditions

In this study, numerical simulations of the three-dimensional flow in the forebay of the pumping station were conducted. The inlet in the numerical model was positioned within the diversion channel sufficiently distant from the forebay's inlet section, aligning with the actual arrangement of the pumping station. The channel was relatively straight, and the velocity inlet boundary conditions were adopted here. The three-dimensional flow simulations within the forebay covered the inlet flow channel. As the flow direction at the outlet section of the inlet channel was unknown, the outlet section of the inlet channel was extended in the section's normal direction, such that the outlet of the inlet channel had a fully developed flow during computation. The outlet of the computational fluid domain was set at a distance of two diameters from the outlet section of the inlet channel, utilizing a free outflow boundary condition. The roughness height was 0.001 m. During the flow field calculation within the forebay, the boundaries of the diversion channel, trash rack bridge piers, the upstream side of the sluice gate, forebay and the walls of the inlet channel were all treated as solid walls by employing logarithmic wall functions. Thermal exchange and conduction between the free surface and air were disregarded for the diversion channel and forebay during the fluid flow computations. The rigid cover assumption was used, and the free liquid surface was adopted as a symmetrical boundary.

2.1.4. Model Meshing and Convergence Analysis

Figure 3 depicts the computational domain adopted for the three-dimensional numerical flow simulations and computational mesh for the flow field in the forebay. Gambit software was employed to partition the computational domain for the numerical flow simulations. Local grids were refined near the channel walls to ensure that the y+ value in the overall computational domain remained below 300, which actually reached approximately 270 at the outlet of the inlet channel. Since a higher number of divisions might affect the accuracy of numerical calculations, the hydraulic loss was taken as an indicator of grid convergence, as presented in Table 3 and Figure 4. The results indicate that when the number of elements in the calculation domain exceeded 5.8 million, the hydraulic loss converged. Therefore, for the following simulations, 6 million elements were adopted.

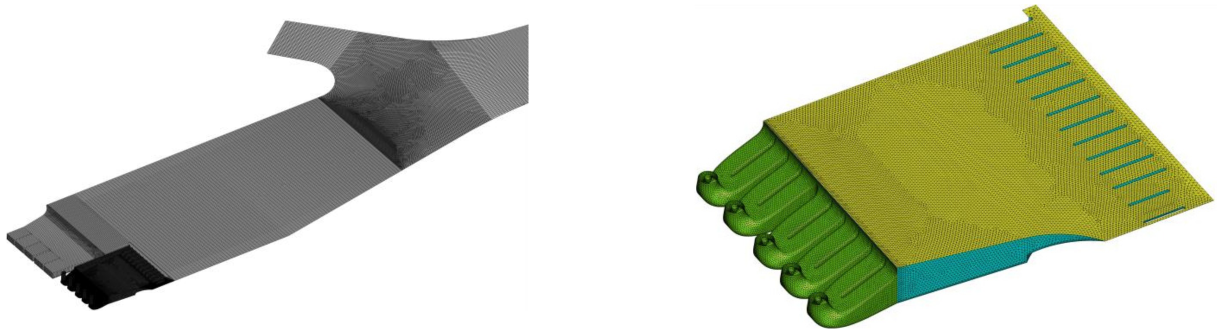

(a) (b)

Figure 3. Numerical mesh. (**a**) Computational domain. (**b**) Forebay.

Table 3. Hydraulic loss under different grid numbers.

Grid Number	2,201,653	2,750,085	3,104,631	3,602,538	4,400,597
Hydraulic loss (m)	0.278	0.267	0.242	0.231	0.223
Grid Number	5,256,840	6,504,713			
Hydraulic loss (m)	0.2191	0.219			

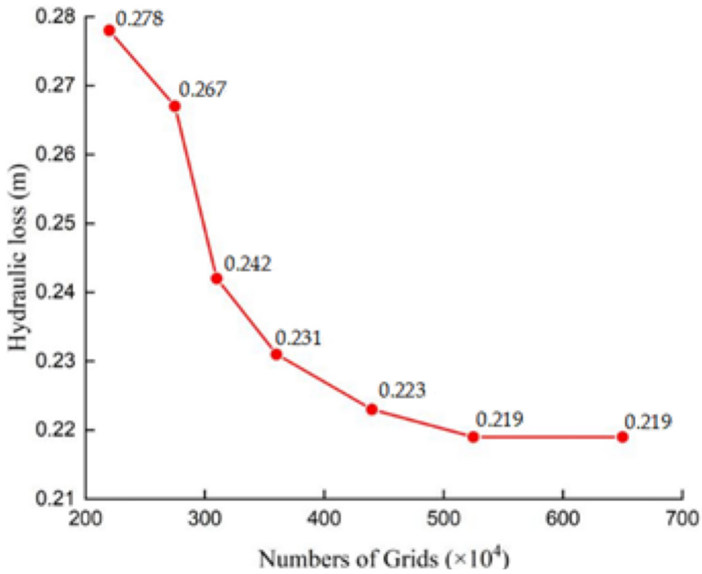

Figure 4. Grid convergence study.

2.2. Model Tests

2.2.1. Experimental Model

Figures 5 and 6 show the layout of the model tests. The regulating sluice of the pumping station had seven openings. Following the parallel arrangement of the sluice gate and pumping station, this study converted the regulating sluice side of the pumping station into the parallel arrangement. The modified prototype included the pumping channel, which was 7 m wide with four inlet flow channels. The regulating sluice comprised three openings, each with a net width of 7 m. The inlet pool was divided into the left and right sides by a 0.8 m wide diversion wall. Looking at the streamwise direction, the left side was defined as the sluice side and the right side as the inlet channel. Inlet channel #1 was near the diversion wall, while inlet channel #4 was close to the wing wall. The modified project included the diversion channel, forebay, inlet channels and the sluice gate.

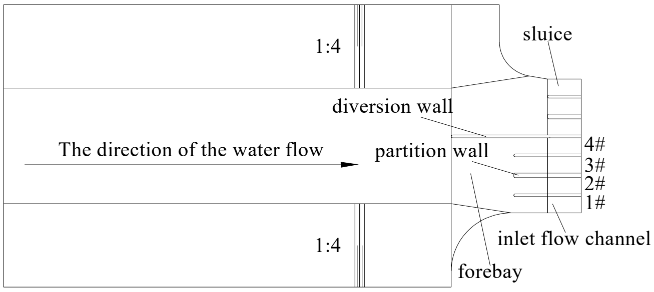

Figure 5. Layout of physical model.

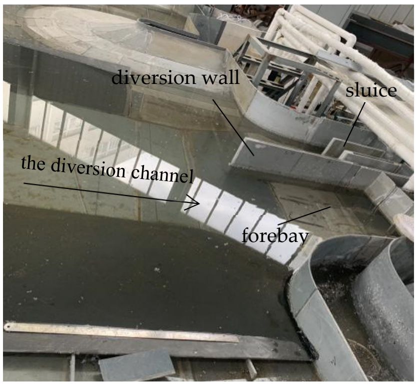

Figure 6. Photo of physical model.

Since gravity was the primary force influencing the water flow in the experiments, gravity similarity was considered. Simultaneously, to ensure that various local hydraulic phenomena in the water flow remained similar, a normal model was used. The design ensured that the gravity similarity maintained the Froude number (F_r):

$$F_r = V_r / \sqrt{g_r l_r} = 1 \tag{6}$$

where V_r is fluid velocity, m/s; g_r is gravitational acceleration, m/s^2; and l_r is characteristic length, m.

Based on the geometric, kinematic and dynamic similarity criteria [24,25], along with relevant regulations, the prototype maximum flow of 100 m^3/s, minimum operational water level of 12.2 m (with a depth of 5.2 m), channel inlet height of 4.452 m, channel inlet width of 7 m and channel inlet submerged depth of 0.75 m was chosen. Based on the dimensions of the pumping station combined with test site conditions, a 1:50 overall normal model was established. According to the similarity criteria, the flow velocity ratio was determined as 7.071, the flow velocity ratio was 17,677.669, and the roughness ratio was 1.919. Following the model roughness criterion [26], considering resistance similarity and prototype roughness (0.011 to 0.020), the corresponding model roughness coefficient ranged from 0.005, 73 to 0.010, 42. The model was fabricated using high-quality polyvinyl chloride (PVC) greyboards (roughness coefficient = 0.007 to 0.010), meeting the test requirements. The overall precision of the model and the fabrication and installation processes complied with the model test specifications.

In order to verify the influence of the partition wall length on the inlet flow regime of a pumping station arranged in parallel with a sluice gate, the changes in hydraulic characteristics between the model test results and numerical simulation results were compared. The model tests, including the physical model and numerical simulation model, were two independent objects; the model and prototype were not consistent. Therefore, the model experiments in this study had certain limitations but further indirectly demonstrated the universality of the proposed measures to improve the inlet flow regime of a pumping station in the forebay.

For these model tests, the four representative operational scenarios #1–4 listed in Table 1 were selected. The operating conditions for these four typical scenarios were as follows: scenario #1 involved the operation of unit #1 only, scenario #2 involved the simultaneous operation of units #1 and 2, scenario 3 involved the simultaneous operation of units #1–3, and scenario 4 involved the simultaneous operation of units #1–4. The four pumping units were sequentially numbered from right to left as #1–4 when viewed in the streamwise direction (Figure 5).

2.2.2. Experimental Methods

Drawing on the numerical calculation results, measures to improve the inlet flow regime were implemented by installing partition walls within the forebay. The wall width corresponded to the width of the separating pier between channels. The wall length was set as twice the width of the inlet channel. The original inlet channel width was 7 m. The wall lengths in the different arrangements were as follows: 0 m in arrangement #1, 7 m in arrangement #2, 14 m in arrangement #3, 21 m in arrangement #4 and 28 m in arrangement #5, respectively. To investigate the flow regime during the operation of the sluice gate and pumping station and the influence of the partition wall length on the inlet flow regime, the tests were carried out using the following methods:

1. Potassium permanganate particles mixed with sand were sprinkled onto the forebay surface to visualize the flow at the bottom of the forebay.
2. The flow velocity at the front of the inlet channel under various conditions was measured using a velocimeter. The data were processed and analyzed to obtain the transverse flow velocity distribution in front of the inlet channel of the pumping station.

3. Analysis of Numerical Simulation Results

3.1. Analyzed Sections

To capture and analyze the internal flow characteristics in the forebay, four sections were selected, as shown in Figure 7. Sections #1 and 2 represent horizontal planes at the surface and bottom layers of the forebay, respectively. Sections 3 and 4 were vertical sections in the upstream and downstream parts of the inlet channel, respectively, and were selected for observing the flow conditions at those locations.

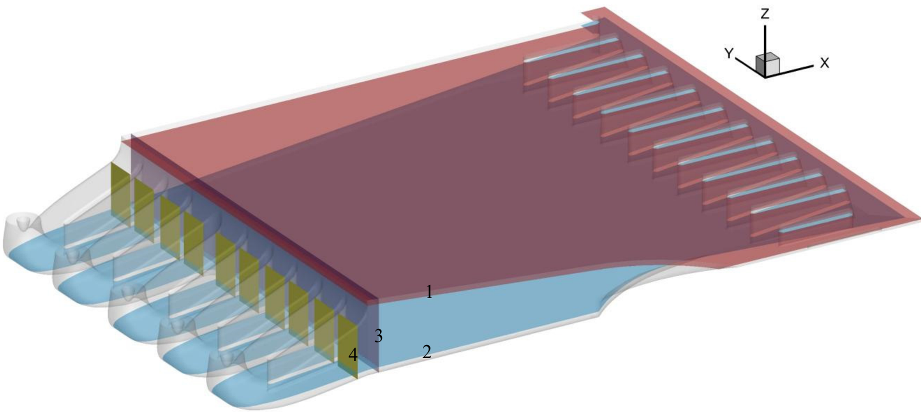

Figure 7. Analyzed sections. Numbers 1–4 represent the section number.

3.2. Flow Field Analysis

Considering different operational combinations and partition wall arrangements, this section presents the flow conditions in the forebay for the most typical operating conditions #1 and 5. Figure 8 illustrates the flow conditions in the forebay for horizontal sections #1 and 2 under operating condition #1. There was an extensive stagnant water body on the sluice side. Influenced by the parallel arrangement of the sluice gate and the station, the influx from the diversion channel flowed at an oblique angle towards the forebay. The water flow on the side away from the diversion wall had a smaller angle and reached the forebay from the diversion channel smoothly. However, closer to the diversion wall, the water flow had a larger tilt angle. The inclined inflow from the diversion channel passed through the trash rack bridge pier before entering the forebay. The bridge partly adjusted the oblique water flow. Without partition walls in the forebay, there was a significant biased flow. There existed a substantial transverse flow in front of the unit #1 inlet channel. Upon the installation of partition walls, a vortex zone appeared on the downstream face at the head of the right partition wall of unit #1. This vortex zone diminished as the length of the partition wall increased. The left opening of the inlet channel witnessed clear improvements in transverse flow compared to arrangement #1, but the right opening of the inlet channel, affected by the vortex zone on the downstream face at the head of the partition wall, showed slightly inferior flow conditions compared to arrangement #1.

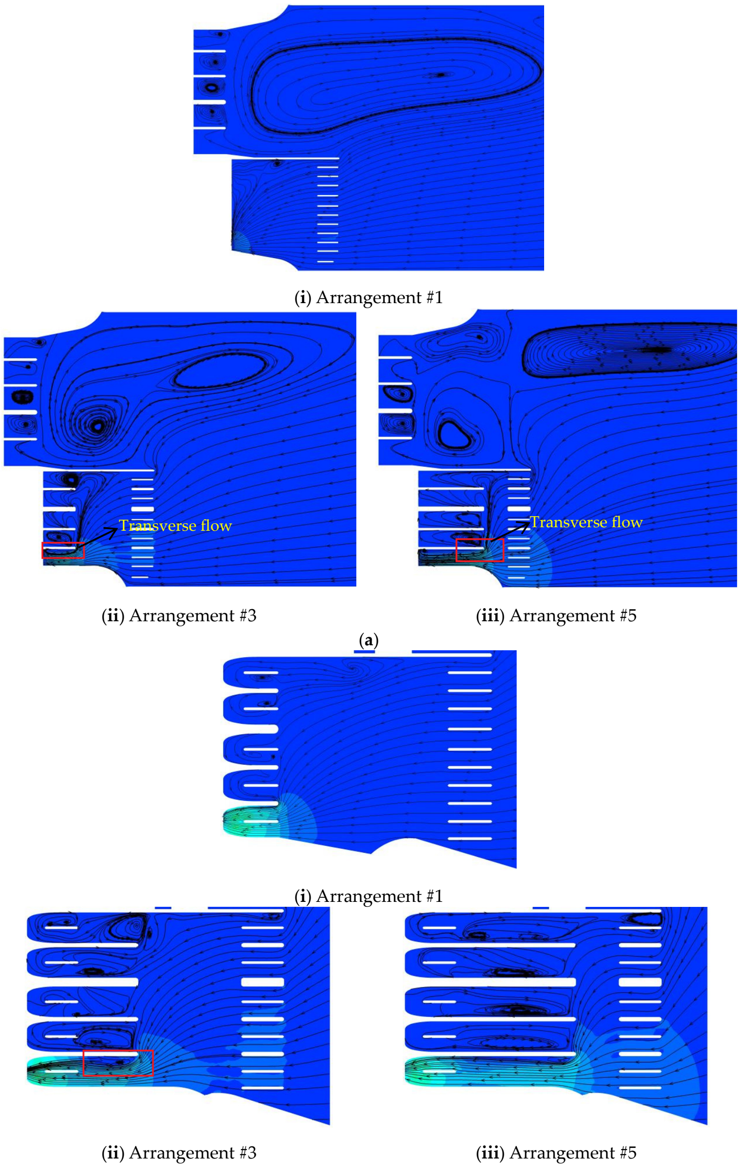

(**i**) Arrangement #1

(**ii**) Arrangement #3 (**iii**) Arrangement #5

(**a**)

(**i**) Arrangement #1

(**ii**) Arrangement #3 (**iii**) Arrangement #5

(**b**)

Figure 8. Horizontal section of forebay flow field (operating condition #1). (**a**) Surface flow field in forebay (section #1). (**b**) Bottom flow field in forebay (section #2).

Figure 9 depicts the forebay flow conditions in horizontal sections #1 and 2 under operating condition #5. The influx from the diversion channel reached the forebay at an oblique angle. On the side away from the diversion wall, the water flow direction after passing through the trash rack bridge appeared relatively straight. However, closer to the diversion wall, a vortex zone emerged on the downstream face at the head of the partition wall due to the combined effect of oblique water flow and the diversion wall. Without partition walls, a transverse flow from left to right occurred within the forebay in the streamwise direction, resulting in a vertical axis vortex in front of unit #5. Further ahead, there was a large vortex zone. As the strength of the vertical axis vortex in the surface layer of inlet channel #5 increased, a suction vortex was produced, attracting pollutants or gases from the water to the channel and pumps. This could potentially impact the safe operation of the pump units. Upon installing partition walls in the forebay, the extensive stagnant water zone on the sluice side was reduced, eliminating the significant biased flow within the forebay. The water, after adjustment by the partition walls, flowed more uniformly into the inlet channel. The flow direction was straight in front of the inlet of the channel, the vertical axis vortex in front of unit #5 inlet channel vanished, and the transverse flow in front of the inlet channel significantly improved compared to the original design.

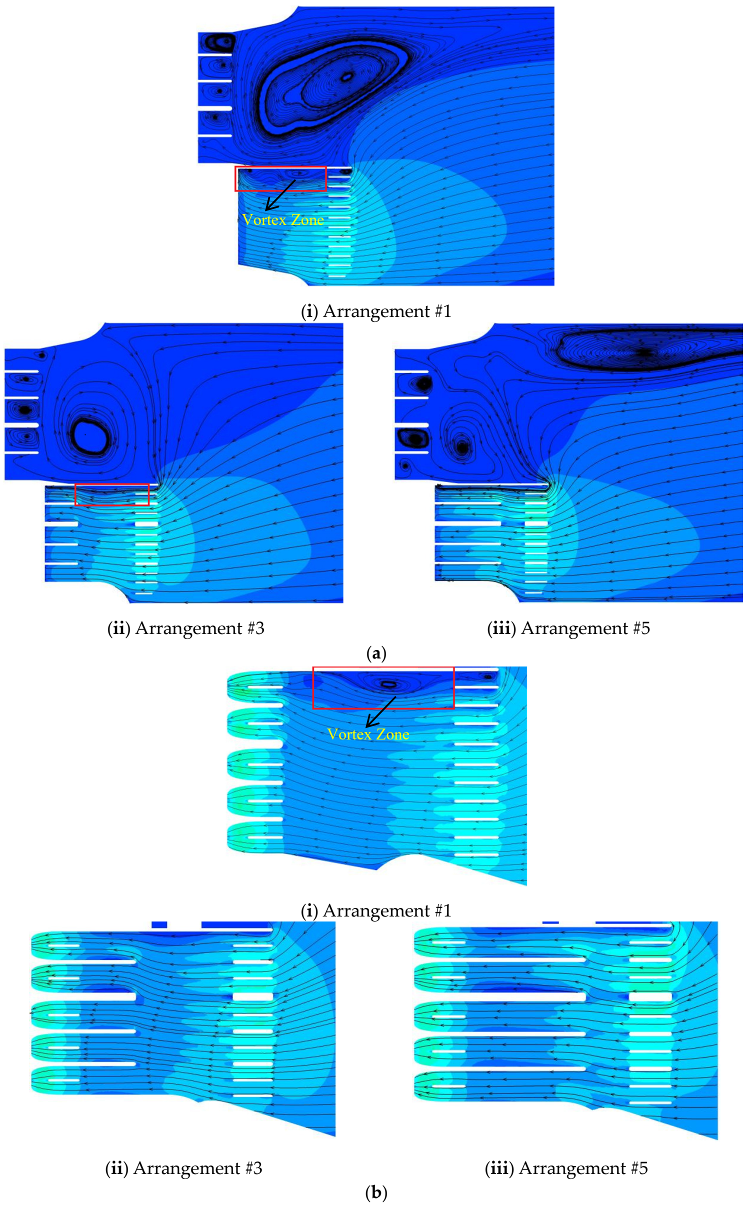

Figure 9. Horizontal section of forebay flow field (operating condition #5). (**a**) Surface flow field in forebay (section #1). (**b**) Surface bottom flow field in forebay (section #2).

3.3. Analysis of Transverse Flow Velocity

Figure 10 compares the transverse flow velocities at the inlet of the channel (section #3) for the six partition wall arrangements. The installation of partition walls in the forebay significantly reduced this transverse flow velocity. The optimal effect was achieved when the wall length was twice the width of the inlet channel (14.2 m). With a further increase in wall length, the transverse flow velocity at the inlet of each channel gradually increased to various degrees. The increase was especially noticeable in front of the inlet channels of the units adjacent to a unit that was not operational.

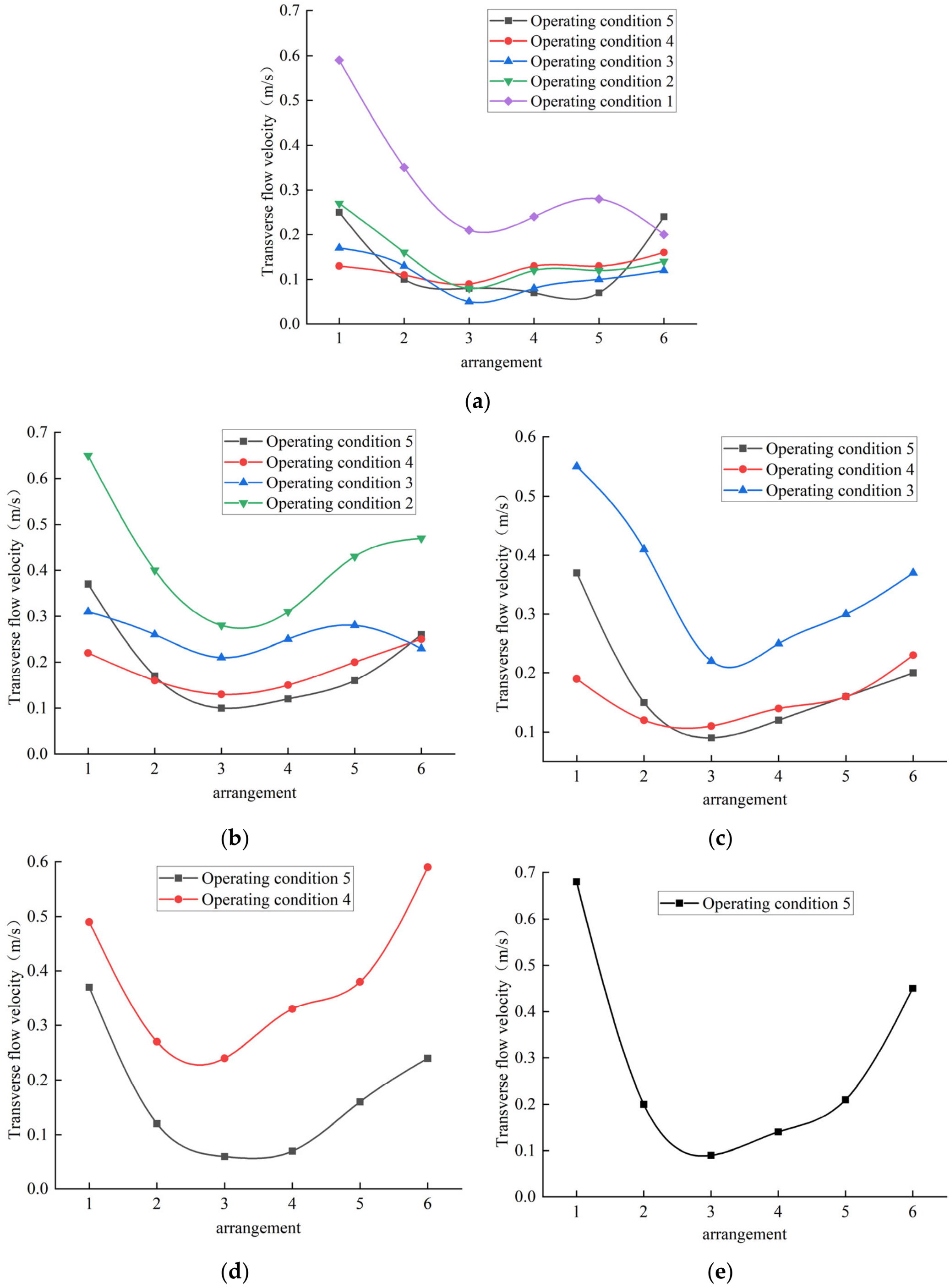

Figure 10. Transverse flow velocities at each channel inlet. (**a**) Unit #1. (**b**) Unit #2. (**c**) Unit #3. (**d**) Unit #4. (**e**) Unit #5.

3.4. Flow Uniformity Analysis

The uniformity of flow velocity distribution [27] can be used to characterize the velocity distributions on the selected characteristic sections. It can be computed as follows:

$$V_u = \left[1 - \frac{1}{\overline{v}_\text{a}} \sqrt{\frac{\left[\sum_{i=1}^{n} (v_{\text{a}i} - \overline{v}_\text{a})^2 \Delta A_i \right]}{A}} \right] \times 100\% \tag{7}$$

where V_u is the relative flow velocity distribution uniformity in the section, $\overline{v}_\text{a}$ is the average axial velocity in the section, v_{ai} is the axial velocity of each calculation unit of the section, and ΔA_i and A are the areas of each calculation unit and the entire section, respectively.

Figure 11 compares the uniformity of flow velocity distribution in the section behind the inlet of the unit inlet channel for six partition wall arrangements (section #4). Separating piers were placed within the straight segment of the elbow-shaped inlet channel of each unit, dividing the inlet of each channel into left and right openings.

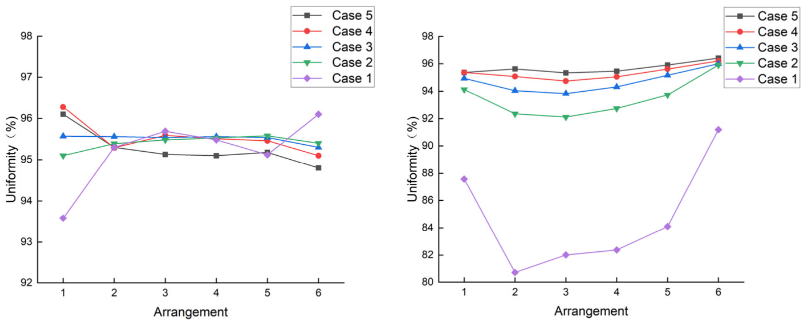

Left opening Right opening

(**a**)

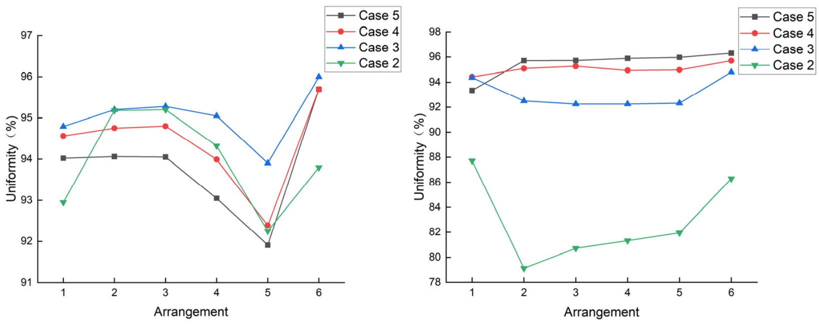

Left opening Right opening

(**b**)

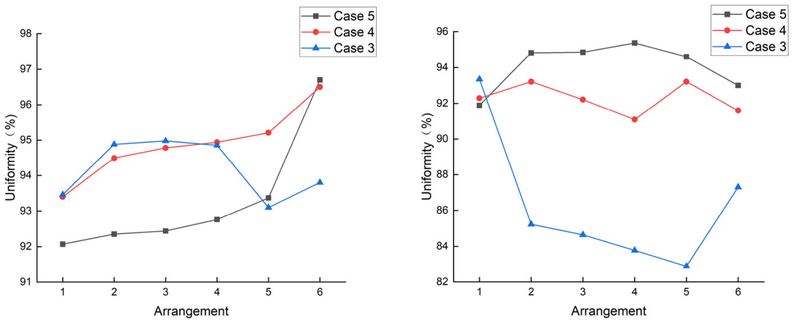

Left opening Right opening

(**c**)

Figure 11. *Cont.*

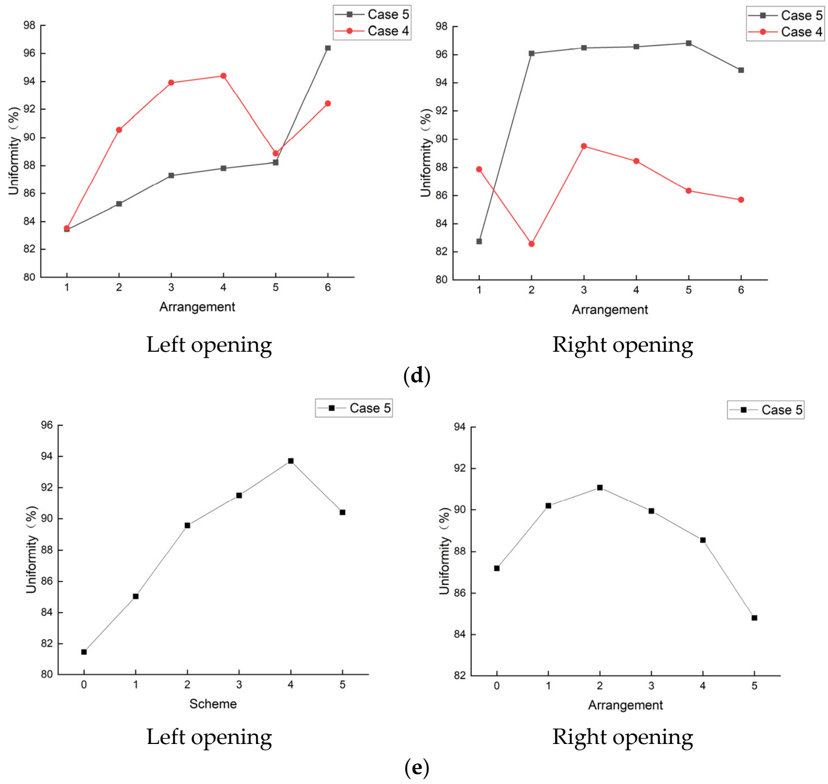

Figure 11. Uniformity of flow velocity distributions behind channel inlets. (**a**) Unit #1. (**b**) Unit #2. (**c**) Unit #3. (**d**) Unit #4. (**e**) Unit #5.

In Figure 11, it can be observed that for unit #1, under operating conditions #2–5, the uniformity of the left and right openings changed only slightly. The uniformity of the left opening decreased with an increase in the length of the partition wall, while that of the right opening increased. In operating condition #1, the uniformity of the right opening was poor. The improvement in uniformity was more apparent in the left opening after adding the partition wall compared to the right opening. However, the uniformity in the right opening decreased after the wall length increased to 7 m, followed by an increase in uniformity with further increases in the wall length.

For unit #2, the uniformity in the left opening reached its optimum wall length of 14 m and decreased with the further increase in the wall length. Then, it significantly increased to a wall length of 48.3 m. The uniformity of the right opening changed slightly under operating conditions #3–5. It decreased at the wall length of 7 m for operating condition #1, then increased with further increases in the wall length.

For unit #3, the uniformity in the left opening increased with an increase in the wall length for operating conditions #4 and 5, while that in the right opening slightly increased at the wall length of 7 m and then decreased with the further increase in the wall length. Under operating condition #3, the uniformity of the left opening reached its optimal level at the wall length of 14 m, while that of the right opening decreased with the increase in the wall length. Both left and right opening uniformities increased again at a wall length of 48.3 m.

For unit #4, both left and right openings reached optimal uniformity at the wall length of 14 m for operating conditions #4 and 5. For unit #5, the uniformity of the left opening increased with the increase in the wall length, while the uniformity of the right opening reached its optimum at the wall length of 14 m.

Considering the transverse flow velocity in front of the channel inlet and the uniformity of flow velocity distribution behind the channel inlets, arrangement #3 (wall length of 14.2 m) was deemed optimal. Compared to arrangement #1, for operating conditions #1 and 2, the uniformity in the left openings of the inlet channels of the operating units improved while the uniformity of the right openings decreased. For operating condition #3, the uniformity changed minimally for the inlet channels of units #1 and 2. There was an increase in uniformity from 93.46% to 94.85% in the left opening of the unit #3 inlet channel and a decrease in uniformity in the right opening. For operating condition #4, minimal changes were observed for the uniformity at the inlet channels of units #1 to 3, while significant improvements were observed in the left opening (from 83.52% to 93.92%) of the inlet channel of unit #4. For operating condition #5, minimal changes occurred for the inlet channels of units #1–3, while apparent improvements were seen for both the left and right openings of the inlet channels of units #4 and 5. Specifically, the uniformity at the left opening of the inlet channel of unit #4 improved from 83.42% to 87.31% and that at the right opening increased from 82.73% to 96.50%, whereas the uniformity at the left opening of the inlet channel of unit #5 improved from 81.47% to 89.57%, and that at the right opening increased from 87.19% to 91.08%.

4. Analysis of Experimental Test Results

4.1. Flow Field Analysis

For the comparison with the numerical simulation results of the forebay flow field presented in Section 3.2, the bottom layer flows of arrangements #1 and 3 were considered. Figure 12 shows the bottom layer flow regime of model test arrangement #1. From the movement of Potassium high monganate granules and sand mixture at the bottom of the forebay, it was observed that during the operation of the units under operating condition #4, a vortex zone existed in front of the inlet of the channel of unit #4, and there was some transverse flow due to the separating piers in front of each unit inlet channel. During the operation of the units under conditions #1–3, a large vortex zone existed within the forebay, which decreased with an increase in the number of operating units. Strong transverse flows were observed in the inlet channels of units adjacent to the inlet of the unit that was not in operation. Operating conditions #1 and 2 produced noticeable disturbances and rotations in the water flow in front of unit #1 and 2 inlet channels, respectively, possibly inducing suction vortices that could affect the safe operation of the pumping units.

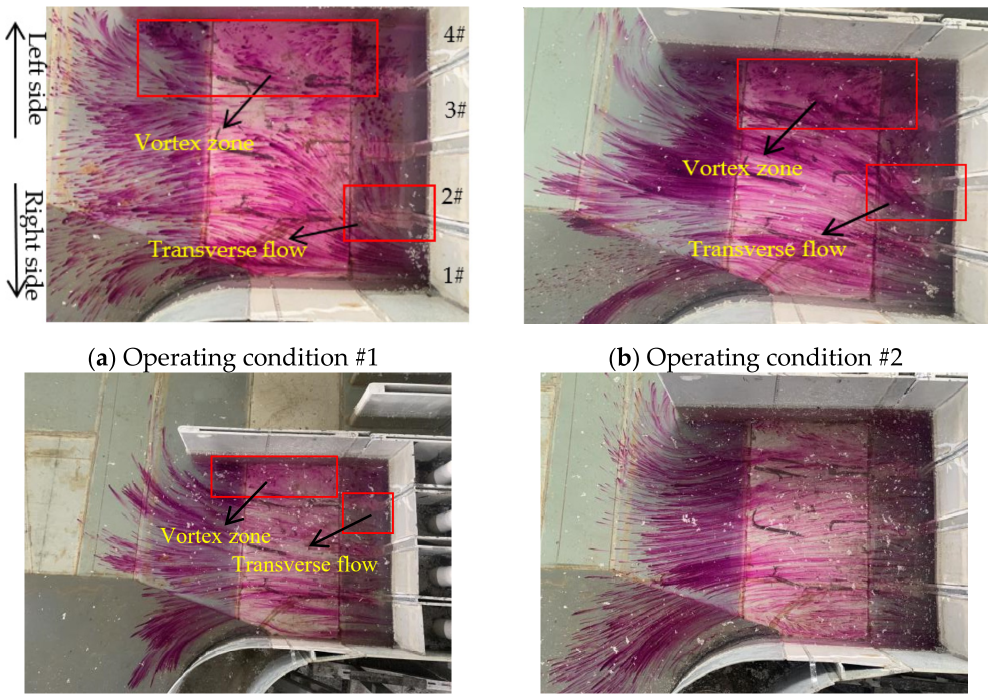

(**a**) Operating condition #1 (**b**) Operating condition #2

(**c**) Operating condition #3 (**d**) Operating condition #4

Figure 12. Flow regime in the bottom layer of forebay in arrangement #1.

Figure 13 shows the bottom layer flow regime of model test arrangement #3. The introduction of partition walls in the forebay improved the flow regime in front of the channel inlet, reducing the transverse flow there compared to arrangement #1. The disturbance and rotation of the water flow were notably reduced in front of the channel inlet of unit #1 during operating condition #1 and in front of the channel inlet of unit #2 under operating condition #2. The flow became more uniform entering the inlet channel, eliminating the primary cause of suction vortices.

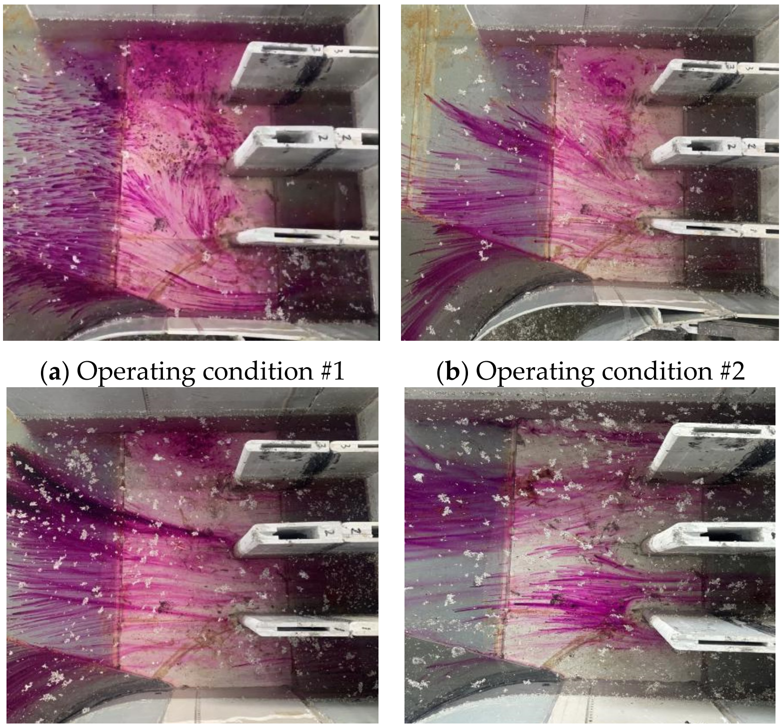

(**a**) Operating condition #1 (**b**) Operating condition #2

(**c**) Operating condition #3 (**d**) Operating condition #4

Figure 13. Flow regime in the bottom layer of forebay in arrangement #3.

4.2. Analysis of Transverse Flow Velocity

The model tests employed the LGY-II intelligent miniature flow velocity meter manufactured by the Nanjing Hydraulic Research Institute. The horizontal position of the measurement point was located in front of the left and right sides of each unit inlet channel. To ensure the accuracy of the transverse flow velocity results, multiple speed measurements were conducted at each measurement point in this experiment. Figure 14 compares the transverse flow velocities at the channel inlet for the five partition wall arrangements. The introduction of partition walls in the forebay significantly impacted the inlet flow regime, greatly reducing the transverse flow velocities at the inlets of the channels. The optimum effect was achieved when the wall length was twice the width of the inlet channel (14 m). With further increases in the wall length, the transverse flow velocities at the inlet of each channel increased to varying extents.

By comparing the experimental and numerical simulation results, it was confirmed that the impacts of different wall lengths on the transverse flow velocity in front of the channel inlet of each pumping unit were generally consistent. The experimental results of the flow direction, biased flow and vortex zone location were also in line with the simulation data. Therefore, the model tests successfully validated the numerical simulation results.

The numerical simulation and model test in this paper have different conditions, but both focus on the influence of the partition wall length on the flow state in front of the inlet channel and obtain the same pattern, which further proves the universality of the proposed measures to improve the inlet flow regime of a pumping station in the forebay.

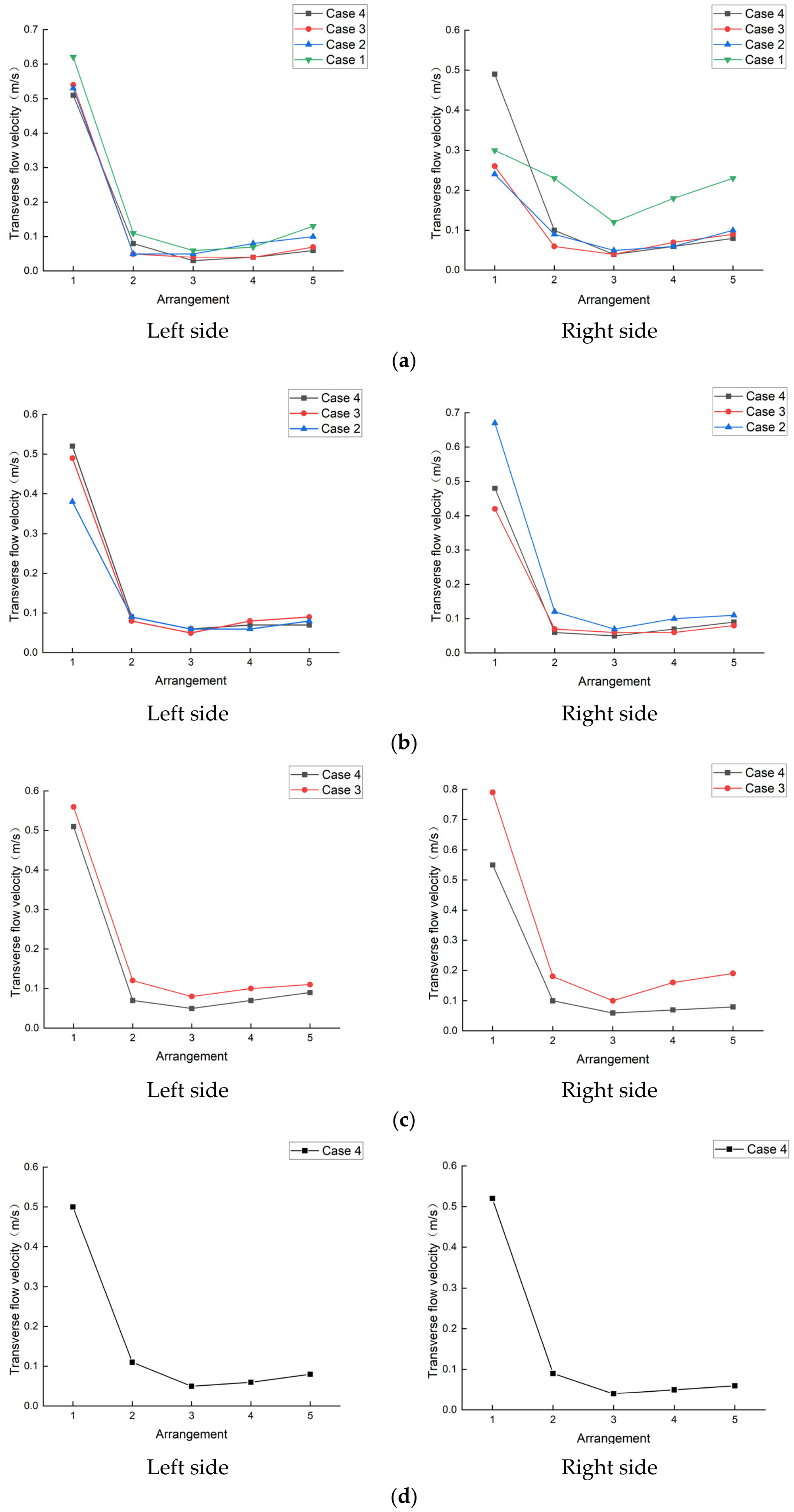

Figure 14. Transverse flow velocities in front of the channel inlets. (**a**) Unit #1. (**b**) Unit #2. (**c**) Unit #3. (**d**) Unit #4.

5. Conclusions

1. During the operation of the pump station arranged in parallel with a sluice gate, there was an adverse flow regime in the forebay. The results of this study can be used to improve the water flow regime in the forebay of pumping stations by introducing partition walls. The additional walls strongly affect the inlet flow regime. The optimum effect was achieved when the wall length was twice the width of the inlet channel, resulting in an average increase of 7.4% in the uniformity of flow velocity distribution at the channel inlet of units #4 and 5.
2. The influence of the length of the diversion wall on the flow of the forebay in the pumping station arranged in parallel with a sluice gate was completed by the methods of the numerical simulation and model test, and the same conclusions were obtained, serving as a reference for the construction of similar pumping stations. Due to the constraints of funds and other conditions, the parameters of the model test and the numerical simulation study in this paper are different, and it is hoped that there will be opportunities to obtain consistent forms of verification in the future.

Author Contributions: Methodology, W.S. and L.X.; software, F.L. and X.Y.; validation, F.L., X.W. and C.N.; formal analysis, W.L. and L.X.; resources, W.S. and X.Y.; writing—original draft, W.S. and F.L.; writing—review and editing, F.L. and L.X.; supervision, X.Y., X.W. and C.N.; project administration, L.X.; funding acquisition, L.X. All authors have read and agreed to the published version of the manuscript.

Funding: This research was funded by the Jiangsu South-to-North Water Diversion Technology R&D Project (JSNSBD202105), the National Natural Science Foundation of China (Grant No. 51779215), and the Jiangsu Water Conservancy Science and technology project (Grant No. 2022010).

Informed Consent Statement: Not applicable.

Data Availability Statement: Data is contained within the article.

Conflicts of Interest: Wei Shi, Xianlei Yu, Xichen Wang and Chun Ni are are employed at Jiangsu Water Supply Co., Ltd. The authors declare no conflicts of interest.

References

1. Shi, W.; Ni, C.; Yu, X.L. Flow pattern improvement in the forebay of pumping station with parallel sluice. *South-North Water Transf. Water Sci. Technol.* **2023**, *21*, 810–820.
2. Lu, Y.J.; Zhou, W.; Ming, Y.M. Layout design optimization of integrated pumping station and sluice with numerical stream simulation. *JDIME* **2014**, *32*, 963–967.
3. Xu, B.; Zhang, C.C.; Xia, H. A Test Research on the Flow Condition Model in Forebay of Pumping Station for Asymmertric Combined Sluice pump Station Project. *Water Resour. Power* **2018**, *36*, 160–162.
4. Xu, C.; Wang, R.; Liu, H.; Zhang, R.; Wang, M.; Wang, Y. Flow pattern and anti-silt measures of straight-edge forebay in large pump stations. *Int. J. Heat Technol.* **2018**, *36*, 1130–1139. [CrossRef]
5. Tang, X.L.; Wang, W.C.; Wang, F.J.; Yu, X.; Chen, Z.C.; Shi, X.Y. Application of LBM-SGS model to flows in a pumping-station forebay. *J. Hydrodyn.* **2010**, *22*, 196–206. [CrossRef]
6. Zang, S.D.; Xu, P.; Dong, Z. Model-test study on improving forebay flow pattern in forward intake pumping station. *Yangtze River* **2019**, *50*, 224–228.
7. Yan, Z.Q.; Gu, J.D.; Zhao, J.J. Experimental study on hydraulic performance Optimization of pump house with ultra-short forebay. *J. Phys. Conf. Ser.* **2021**, *2044*, 12020. [CrossRef]
8. Zhang, X.W.; Liu, C.; Rong, Y.C. Numerical simulation and experimental verification of forward feed array diaphragm rectifier for multi-unit pumping station. *J. Drain. Irrig. Mach. Eng.* **2021**, *40*, 378–384.
9. Feng, T.T. Improvement of Drift in Side-Intake of Suction Intank Canal and Optimization of Parameters of Curved Wing Walls. Master's Thesis, Yangzhou University, Yangzhou, China, 2021.
10. Teaima, I.R.; EI-Gamal, T. Improving Flow Performance of Irrigation Pump Station Intake. *J. Appl. Water Eng. Res.* **2017**, *5*, 9–21. [CrossRef]
11. Zi, D.; Wang, F.; Yao, Z.; Hou, Y. Effects analysis on rectifying intake flow field for large scale pumping station with combined diversion piers. *Trans. Chin. Soc. Agric. Eng.* **2015**, *31*, 71–77.
12. Luo, C.; Qian, J.; Liu, C. Numerical simulation and test verification on diversion pier rectifying flow in forebay of pumping station for asymmetric combined sluice-pump station project. *Trans. Chin. Soc. Agric. Eng.* **2015**, *31*, 100–108.

13. Wang, H.D.; Tai, Y.J.; Huang, L.X. Analyzing Water and Sediment Flow Patterns in Circular Forebays of Sediment-Laden Rivers. *Sustainability* **2023**, *15*, 16941. [CrossRef]
14. Song, W.W.; Pang, Y.; Shi, X.H. Study on the Rectification of Forebay in Pumping Station. *Math. Probl. Eng.* **2018**, *1*, 1–16. [CrossRef]
15. Xia, C.Z.; Cheng, L.; Jiao, W.X. Nurnerical simulation on rectification measure of inverted T-shaped sill at forebay of pump station. *South-North Water Transf. Water Sci. Technol.* **2018**, *16*, 146–150+163.
16. Zhou, M.; Zhou, C.F.; Zhou, Y.X. Influence of circular columns on flow pattern in side-intake forebay of pumping station and rectification mechanism. *J. Yangzhou Univ.* **2020**, *23*, 73–78.
17. Yu, Y.H.; Yan, H.D.; Ye, C.L. Parameter optimization of rectification sill in the forebay of pumping station using BPNN-GA algorithm. *Trans. Chin. Soc. Agric. Eng.* **2023**, *39*, 106–113.
18. Luo, C.; Cheng, L.; Liu, C. Numerical simulation of mechanism for sill rectifying flow in pumping station intake. *J. Drain. Irrig. Mach. Eng.* **2014**, *32*, 393–398.
19. Xu, P.F.; Chen, Y.C.; Xu, G.Y. Experimental analysis of Xihe pumping station under asymmetric operation. *South-North Water Transf. Water Sci. Technol.* **2024**, *22*, 1–8.
20. Han, F.; Liang, J.D. Numerical Simulation and Improvement for Flow Pattern in Forebay of One-way Inflow Pumping Station. *China Rural. Water Hydropower* **2018**, *8*, 190–193.
21. Ying, J.W.; Yu, X.D.; He, W. Volume of fluid model-based flow pattern in forebay of pump station and combined rectification scheme. *J. Drain. Irrig. Mach. Eng.* **2020**, *38*, 476–480.
22. Nasr, A.; Yang, F.; Zhang, Y.Q. Analysis of the Flow Pattern and Flow Rectification Measures of the Side-Intake Forebay in a Multi-Unit Pumping Station. *Water* **2021**, *13*, 2025. [CrossRef]
23. Zheng, X.B.; Zhang, P.L.; Zhang, W.J. Numerical Study on the Influence of Combined Rectification Facilities on the Flow in the Forebay of Pumping Station. *Water* **2023**, *15*, 3847. [CrossRef]
24. Zhu, H.G.; Xi, B. New method for pump sump hydraulic medel study. *Trans. Chin. Soc. Agric. Mach.* **2023**, *34*, 72–75.
25. *ANSI/HI 9.8-2018*; Rotodynamic Pumps for Pump Intake Design. Hidraulic Institute: Parsippany, NJ, USA, 2018.
26. Sun, D.X.; Mu, Z.W.; Li, F.Q. Experimental study on hydraulic characteristics of diversion pier combined with rough-strips energy dissipator in the bend spillway. *J. Water Resour. Water Eng.* **2019**, *30*, 166–171.
27. Zhou, D.F.; Wang, Y.B.; Zhou, J.R. Optimization of numerical simulation for intake sump in a sluice-pump station. *Hydro-Sci. Eng.* **2023**, *5*, 68–77.